

# Micro-Cavity in Organic Light-Emitting Diode

Young-Gu Ju  
*Department of Physics Education, Kyungpook National University  
 Korea*

## 1. Introduction

The study on micro-cavity in organic light-emitting diode(OLED) demands understanding the theory of multi-layer films. It is because OLED is basically an optical device and its structure consists of organic or inorganic layers of sub-wavelength thickness with different refractive indices. When the electron and holes are injected through the electrodes, they combine in the emission layers emitting the photons. These photons will experience the reflection and transmission at each interface and the interference will determine the intensity profile. The light reflected at the interfaces or the metallic electrode returns to the emission layer and affects the radiation efficiency. In optical terminology, OLED belongs to a micro-cavity being comprised of multi-layers. Therefore, before studying the cavity effect of OLED, we better begin with the theory of multi-layer film theory in optics. This theory is well explained in most of textbook dealing with optics since it relates to optical coatings and lasers(Fowles, 1975; Born & Wolf, 1989). In this section, a brief review will be given for the purpose of self-containment, which will be especially helpful for the beginners.

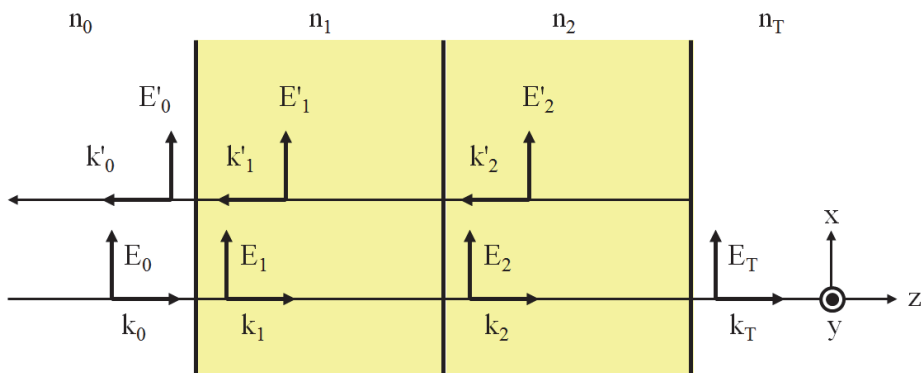


Fig. 1. The schematic diagram of multi-layer and the electric fields inside the film

The four layers and the electric fields are displayed in Fig. 1. For the time being, the four layers are called as the zero-th, the first, the second and the final layer, respectively. A plane wave designated  $E_0$  with propagation vector of  $k_0$  is normally incident on the first layer from the zero-th layer and generates the reflected electric field designated by  $E'_0$  with  $k'_0$ .

The first medium also contains two electric fields  $E_1$  and  $E_1'$ .  $E_1$  and  $E_1'$  represents the electric fields measured at the first interface between the zero-th medium and the first medium.  $E_2$  and  $E_2'$  also represents the electric fields travelling in positive and negative z-direction, which is also measured at the second interface. The final layer has only one electric field  $E_t$  since it doesn't have a reflection.

In terms of geometrical optics, the reflection occurs infinite times between the interfaces. However, in this type of analysis, all those rays are summed up into two electric fields in each medium. In other words, the electric fields propagating in positive and negative z-direction already take into account of multiple reflections. In this configuration, the final amplitude of the electric field is obtained by applying the boundary condition at each interface. The boundary conditions used in the calculation requires that the E field component and H-field component parallel to the interface should be continuous at the interfaces. If these boundary conditions apply to the interface between the first medium and the second medium, the following equations hold.

$$E_1 e^{ikl} + E_1' e^{-ikl} = E_2 + E_2' \quad (1)$$

$$H_1 e^{ikl} + H_1' e^{-ikl} = H_2 + H_2' \quad (2)$$

The electric  $E_1$  has the extra phase factor of  $\exp(ikl)$  since it propagate further in z direction by the layer thickness  $l$ . In addition, H field satisfies the following relation with E field.

$$\vec{H} = \frac{1}{\mu\omega} \vec{k} \times \vec{E} \quad (3)$$

The propagation vector  $k$  is equal to the product of refractive index  $n$  and the propagation vector  $k_0$  in vacuum. The amplitude of H field is proportional to E field and refractive index  $n$  since the  $k_0$ , permeability  $\mu$  and angular frequency  $\omega$  do not depend on the medium when the medium is non-magnetic. In this manner, Eq. 2 becomes Eq. 4.

$$n_1 E_1 e^{ikl} - n_1 E_1' e^{-ikl} = n_2 E_2 - n_2 E_2' \quad (4)$$

In general, the subscript denoting the layer number can be replaced by  $i$ . For instance, the number 1 can be changed into  $i$  and the number 2 can be  $i+1$ , representing  $i$ -th and  $(i+1)$  th layer, respectively. The two equations with the new indices are expressed in Eq. 5, and Eq. 6.

$$E_i e^{ik_i l_i} + E_i' e^{-ik_i l_i} = E_{i+1} + E_{i+1}' \quad (5)$$

$$n_i E_i e^{ik_i l_i} - n_i E_i' e^{-ik_i l_i} = n_{i+1} E_{i+1} - n_{i+1} E_{i+1}' \quad (6)$$

The two special cases for this general iteration formula occur at the first interface and the last one. The first layer and the final layer have zero thickness so that exponential factors become 1. Moreover, the final layer doesn't have the reflected wave so that the second term on the right hand side of equation should disappear. The conversion of the equations into the neater forms can be done using a matrix.

$$\begin{pmatrix} e^{ik_i l_i} & e^{-ik_i l_i} \\ n_i e^{ik_i l_i} & -n_i e^{-ik_i l_i} \end{pmatrix} \begin{pmatrix} E_i \\ E_i' \end{pmatrix} = \begin{pmatrix} 1 & 1 \\ n_{i+1} & -n_{i+1} \end{pmatrix} \begin{pmatrix} E_{i+1} \\ E_{i+1}' \end{pmatrix} \quad (7)$$

$$\begin{pmatrix} E_i \\ E_i' \end{pmatrix} = \begin{pmatrix} e^{ik_i l_i} & e^{-ik_i l_i} \\ n_i e^{ik_i l_i} & -n_i e^{-ik_i l_i} \end{pmatrix}^{-1} \begin{pmatrix} 1 & 1 \\ n_{i+1} & -n_{i+1} \end{pmatrix} \begin{pmatrix} E_{i+1} \\ E_{i+1}' \end{pmatrix} = A_{i+1} \begin{pmatrix} E_{i+1} \\ E_{i+1}' \end{pmatrix} \quad (8)$$

$$\begin{pmatrix} E_0 \\ E_0' \end{pmatrix} = A_1 A_2 \cdots A_N \begin{pmatrix} E_T \\ 0 \end{pmatrix} \quad (9)$$

From the matrix formula, we can see more clearly the evaluation process of the electric field in the multi-layer films. If we set the final goal to finding the reflectivity of the films when looking on the first layer, the problem is equivalent to evaluating the ratio of  $E_0'$  to  $E_0$ . According to Eq. 8,  $E_0$  fires the next sequence by multiplying  $A_1$  and  $(E_1, E_1')$ . Since  $A_1$  can be obtained using the index and the thickness of the layer, the problem is finding out  $E_1$  and  $E_1'$ . The  $E_1$  and  $E_1'$  can be calculated by finding out  $E_2$  and  $E_2'$ . In this way, the iteration continues until it reaches the final layer. At the final layer,  $E_t$  and  $E_t'$  should be given somehow. The solution is rather simple.  $E_t'$  is 0 and  $E_t$  can be any value, for example, 1. The matrix equations express  $E_0$  and  $E_0'$  as a ratio to  $E_t$  anyway. However, the reflectivity is again the ratio of  $E_0'$  to  $E_0$  so that the absolute value doesn't affect the answer no matter what value we choose for  $E_t$ . If someone insists on the absolute value of  $E_0$  and  $E_0'$ , then the  $E_0$  and  $E_0'$  are evaluated in the unit of  $E_t$ . Since  $E_0$  is given as an input value, the  $E_t$  is adjusted to make  $E_0$  equal to the given input value. This  $E_t$  also can be used to get the absolute value for  $E_0'$ .

## 2. Programming the multi-layer equations in MATLAB

In this section, we present a MATLAB code to calculate the electric field and the reflectivity inside the multi-layers. This approach will provides a realistic view on the field profile inside the cavity and how it affects the optical property by giving a numerical value in a concrete example. Among many programming languages, MATLAB is chosen since it is a high level language. Programmers usually don't have to worry about the details of matrix manipulation, complex variable, graphics and so on. From an educational viewpoint, the code in MATLAB is easy to explain.

( FILE: MLay.m )

```
clear all;
global Nm;
global rfr;
global MA;
global Efl;
wvl = 0.5; % in um
rfr = [1.0 2.5 1.5 2.5 1.5 2.5 1.0];
thick = wvl./(4*rfr);
Nm = length(rfr);
thick(1) = 0;
thick(Nm) = 0;
kv = 2*pi*rfr/wvl;
MA = @(k) [exp(i*k*kv(k)*thick(k)), exp(-i*k*kv(k)*thick(k));
rfr(k)*exp(i*k*kv(k)*thick(k)), -rfr(k)*exp(-i*k*kv(k)*thick(k))];
Efl=[];
```

```

vEf = Ef(1);
[thl2, Efl2, intfl2] = EProf(Efl,kv,thick);
Instl2=abs(Efl2).^2;
plot(thl2, Instl2, 'r-', thl2(intfl2), Instl2(intfl2), 'bO');
R = abs(vEf(2)/vEf(1))^2

```

The program consists of three script files. The codes of “MLay.m” are presented above. The lines of “Ef.m” and “EProf.m” are also presented in the following. The input parameters such as wavelength, refractive index and thickness of the layers are set in the first program. The variables corresponding to these input parameters are “wvl”, “rfr” and “thick”. It is worthy to note that the first layer and the final layer are the zero-th layer (incident medium) and the transmission medium as described in Fig. 1. The thicknesses of those two layers are set to 0. The thicknesses of the layers are set to be a quarter wavelength as a starting example. These values can be changed complying with the user’s need. The other variation is found in the indexing of the array variable. The initial index of the array in MATLAB is 1 instead of 0, which is different from Eq. 8. The main calculation is performed in the definition of “MA” and the “Ef(1)”. Ef(1) calls the function routine defined in the separate script file “Ef.m”. It is an execution of iteration formula Eq. 8. When it reaches the final layer, it is given the final numerical value 1.0 for the electric field at the final medium and returns to the previous function calls, consecutively. All the readers have to do is to put these three files in a MATLAB current folder and run “MLay.m”.

( FILE: Ef.m )

```

function [z]=Ef(k)
global Nm;
global rfr;
global MA;
global Efl;
if(k == Nm)
z=[1.0; 0.0];
else
z=inv(MA(k))*[1 1;rfr(k+1) -rfr(k+1)]*Ef(k+1);
end
Efl = [transpose(z); Efl];
end

```

( FILE: EProf.m )

```

function [thl2, Efl2, intfl2] = EProf(Efl, kv, thick)
Ndiv = 10;
Nm = length(thick);
cth0 = cumsum(thick);
Efl2 = [Efl(1,1)+Efl(1,2)];
thl2 = [cth0(1)];
intfl2 = [1];
for n=2:(Nm-1)
cth = [0:thick(n)/Ndiv:thick(n)];
Efl_tmp = Efl(n, 1)*exp(i*kv(n)*cth)+Efl(n, 2)*exp(-i*kv(n)*cth);
Efl2 = [Efl2, Efl_tmp];
thl2 = [thl2, cth0(n-1)+cth];
intfl2 = [intfl2, length(thl2)];

```

```

end
Efl2 = [Efl2, [Efl(Nm,1)+Efl(Nm,2)]];
thl2 = [thl2, cth0(Nm-1)+thick(Nm)];
end

```

Finally, the “EProf.m” is in charge of calculating the field profile at the interfaces and the between them. The E field is assumed to vary in accordance with the plane wave solution. In other words, the electric field amplitudes evaluated at the interfaces are used to give the value between them. The results are plotted using “plot” function and the reflectivity of the multi-layers is calculated from the  $E_0$  and  $E_0'$ .

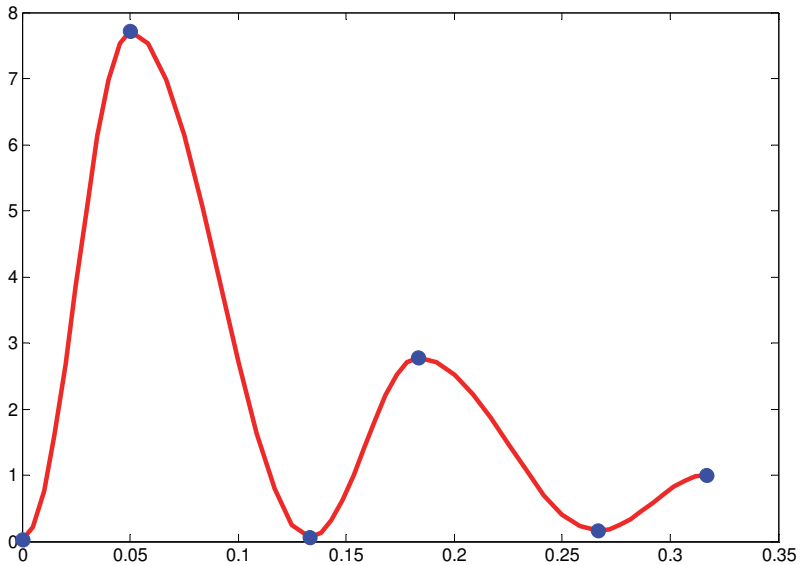


Fig. 2. The output from the execution of the program “MLay.m” is displayed.  $R = 0.9204$ . The refractive index and the thickness for input are

```

“rfr = [1.0 2.5 1.5 2.5 1.5 2.5 1.0];”
“thick = wvl./(4*rfr);”
“thick(1) = 0;”
“thick(Nm) = 0;”

```

The result of execution is shown as in Fig. 2. In this simulation, the layer structure is comprised of air, 2.5 pairs of TiO<sub>2</sub>/SiO<sub>2</sub>, and air from the incident medium. The final reflectivity of the layers is about 92 %. The thickness of each layer is a quarter wavelength to obtain the high reflection. The circular marks represent the position of the interfaces so that the region between the marks corresponds to a single layer. Since the incident medium and the final medium have zero thickness, the number of layers seen in Fig. 2 is only 4 instead of 6. The peak intensity decreases as the light penetrates the layers.

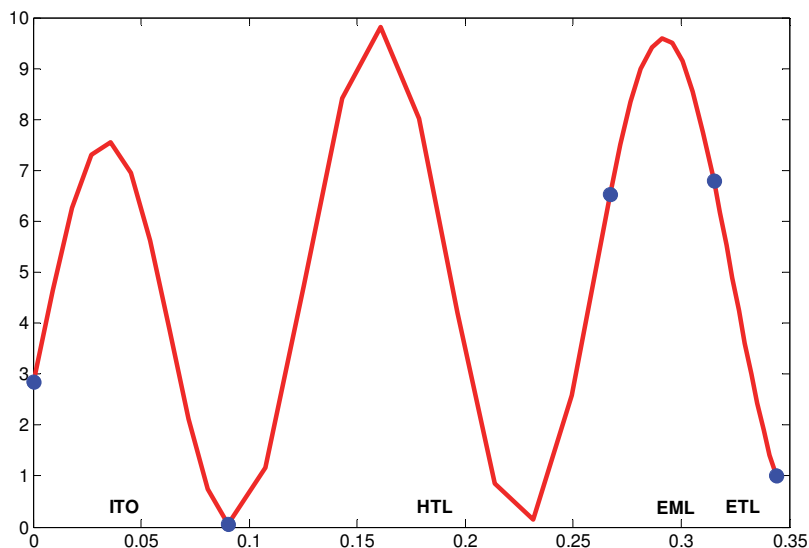


Fig. 3. The output from the execution of the program “MLay.m” is displayed.  $R = 0.8706$ . The refractive index and the thickness for input are

“rfr = [1.5 2.13 1.87 1.94 1.75 0.644+5.28i];”

“thick = [0 0.09 0.177 0.048 0.029 0];”

In order to analyze of the real OLED device, the refractive index and the thickness are replaced by those of the OLED. The layers used in the simulation are overcoat, indium tin oxide(ITO), hole transport layer(HTL), emission layer(EML) and aluminum cathode, respectively. The title of each layer is typed in as an annotation at the bottom of the plot between the circular marks, which represent the boundaries of each layer. The light is supposed to be incident on the overcoat layer first.

In the design of the OLED cavity, the position of the emission layer is important since it affects the emission efficiency of the device. As in Fig. 3, the emission layer occupies the peak position of the intensity profile. It means that the optical density of state is high over the emission layer and the electron transition rate is also high. If the emission layer is placed around the node of the intensity profile, the spontaneous emission is suppressed rather than enhanced. Quantum mechanics states that the radiation probability is proportional to the electron transition probability and the optical density of states(Gasiorowicz, 1984). If the two atoms have the same transition probability, but have different optical density of states, which generally depends on the position of the atom inside the cavity, the resultant transition rate comes to be determined by the optical density around the atom. This kind of enhancement is often observed in the design of a micro-cavity laser such as vertical-cavity surface-emitting laser(VCSEL). Therefore, the OLED engineer should pay attention to controlling the thickness of the layers so that the emission layer is positioned at the peak of the intensity, otherwise, he will lose optical efficiency.

Eq. 8 can be modified into a bit more complicated form in order to handle oblique incidence angle, polarization, dispersion, user-friendly interface, and so on. But, all these variations stick around the same boundary conditions under different circumstances. The generalization of the program is left for the fun of the reader.

### 3. Tunable micro-cavity in OLED

In the former section, the MATLAB program calculates the electric field profile inside the conventional OLED device. The multi-layer structure naturally forms the cavity through the reflections at the interfaces of the cathode, organic layers, anode, and so on. The bandgap difference between the materials causes the index differences and this index mismatch accompanies reflections. Therefore, it is very hard to get rid of the reflections at the interfaces and the cavity effect inside the OLED. In this section, we present the method of how to more actively use this interference in order to control the emission wavelength of the white OLED.

The design of a strong cavity can be realized by reinforcing the bottom mirror. In the conventional OLED, the anode usually consists of a transparent conductive oxide like indium zinc oxide(IZO) and it plays a role of bottom mirror. The higher index contrast between IZO and the neighboring layers increases the reflectivity at the interfaces. Since Al cathode already keeps high reflectance over the visible wavelength, increasing the reflectivity of the bottom mirror can strengthens the cavity effect. At first thought, a metallic layer at the bottom can be used to make a strong cavity. However, metals usually have a very high imaginary index, which means strong absorption. In this case, the light generated inside cannot escape the cavity unless the metallic layer is very thin. As matter of fact, very thin layer of silver can forms the strong cavity in OLED. However, the thin layer is not easy to deposit maintaining the uniformity of the device.

In this article, we present the results in which distributed Bragg reflector(DBR) comprises the bottom mirror of the cavity. The DBR is simply a periodic stack of dielectrics with different refractive index. The thickness is usually a quarter wavelength to increase the reflectivity. The schematic diagram of the micro-cavity consisting of DBR is displayed as in Fig. 4. Compared to the structure used in the simulation for Fig. 3, the bottom side has three additional layers of IZO/SiO<sub>2</sub>/IZO. Although these three layers seem to lack the number of layers comparing to the DBR in VCSELs, this number of layers are adequate for controlling the emission property of the OLED.

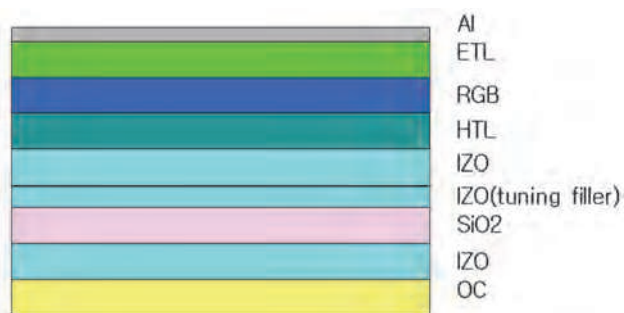


Fig. 4. The structure of strong cavity used for controlling the emission wavelength of white OLED.

It is worthy to note that the thickness of the second IZO layer is variable to tune the resonant wavelength. In general, the resonant peak moves depending on the thickness of the cavity. In a conventional cavity, the central layer such as the emission layer in this structure is adjusted to change the resonance. However, the emission layer in OLED is kind of sensitive layer which should be untouched due to the optimization of the emission characteristics. Instead, the extra tuning layer is added to the anode layer to affect the cavity length. This technique is often used to make a tunable VCSEL (Ju et al, 2000).

The analysis of the cavity effect needs the information on the spectral reflectance. The program used in the previous section should be modified to calculate the reflectivity over a range of wavelength instead of a single wavelength. The modified code is shown below.

( FILE: M Lay\_a2.m )

```
clear all;
global Nm;
global rfr;
global MA;
global Efl;
wvli=0.4;
wvlf=0.7;
wvlwd=0.002;
rfr = [1.5 2.1+0.016i 1.5 2.1+0.016i 2.13 1.87 1.94 1.75 0.644+5.28i];
thick = [0 0.073 0.089 0.040 0.09 0.117 0.048 0.029 0];
Nm = length(rfr);
thick(1) = 0;
thick(Nm) = 0;
wvll = [wvli:wvlwd:wvlf];
Rcurve=[];
for n=1:length(wvll)
wvl=wvll(n);
kv = 2*pi*rfr/wvl;
MA = @(k) [exp(i*kv(k)*thick(k)), exp(-i*kv(k)*thick(k));
rfr(k)*exp(i*kv(k)*thick(k)), -rfr(k)*exp(-i*kv(k)*thick(k))];
vEf = Ef(1);
Rcurve = [Rcurve; [wvl*1000, abs(vEf(2)/vEf(1))^2]];
end
plot(Rcurve(:, 1), Rcurve(:,2));
grid on;
xlabel('wavelength(nm)');
ylabel('reflectivity');
```

The outcome of the program is displayed in Fig. 5. This modelling assumes that the tuning layer is 40 nm IZO. The reflectance has its resonance at 540 nm. The rapid drop of reflectivity at the center indicates that the transmission is high at this wavelength. This is a typical behavior of a cavity made with two highly reflecting mirrors. Although the mirror reflects the incident light, the constructive interference inside the cavity under resonant condition makes the transmission very high. Although the simulation calculates the reflectivity curve, it also provides the information about the spectral emission. The transmittance or the spectral emission can be obtained by subtracting reflectance from 1. Therefore, the spontaneous emission other than the resonant wavelength is suppressed by



the cavity. If the emission layer contains the RGB emission layer as in white OLED, the resonant wavelength determines the emission color of the pixel. As for 40 nm IZO tuning layer, the cavity allows the pixel to emit 540 nm with spectral width of 50 nm, which is narrower than the natural spectral width of the green emission in OLED. In other words, the use of cavity enhances the color purity of the emission.

For the most part, OLED includes color filter(CF) layer to reduce the spectral width and improve color gamut. However, the reduction of spectral width comes through the absorption of the light energy outside the spectral window of the pigment. It suffers energy loss for the sake of enhancement in color purity. On the contrary, the spectral narrowing induced by cavity effect doesn't suffer energy loss since it originates from the change of optical modes inside the cavity, not the absorption process. Therefore, the cavity in OLED increases the transmission efficiency through CF by narrowing the spectral width without energy loss.

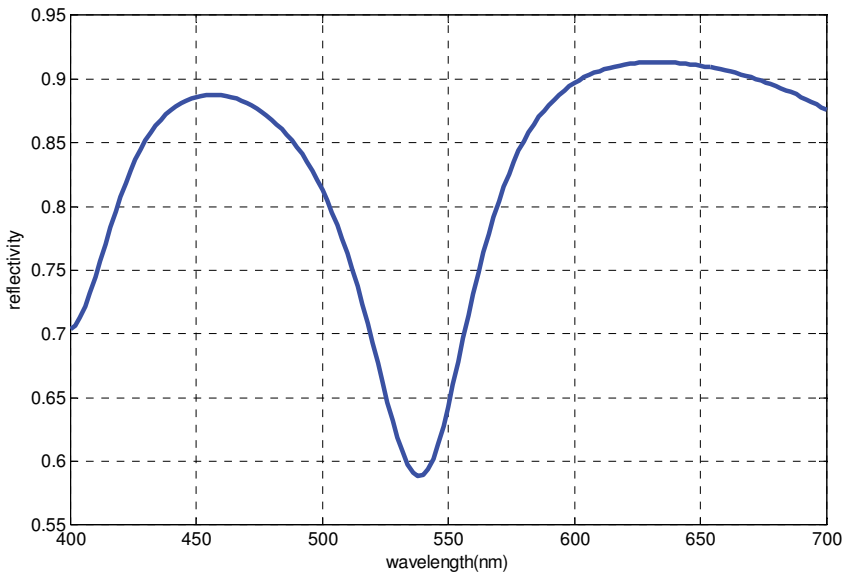


Fig. 5. The reflectivity curve is calculated when the tuning layer is IZO and 40 nm thick.

Furthermore, the resonance in this DBR cavity varies as a function of the thickness of the tuning layer. As the thickness of the tuning layer increases, the resonance shifts toward long wavelength. When the tuning IZO layer is 100 nm, the resonance goes from 540 nm to 620 nm and the secondary resonance appears at 460 nm as seen from Fig. 6. The thicker tuning layer provides the way to narrow the spectral width of blue and red emission. It means that one tuning layer can create two resonances at the same time. In this way, two types of tuning layers can make the interference filter for RGB and enhance the optical efficiency in OLED. The reflectivity curves with different tuning layer and thickness are shown in Fig. 7. It shows that SiN<sub>x</sub> also function as a tuning layer but with smaller spontaneous enhancement due to its smaller index.

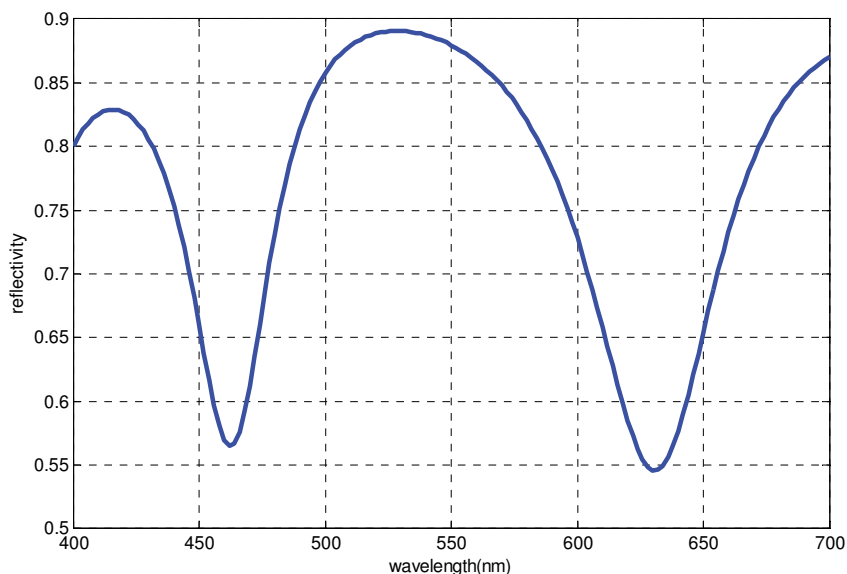


Fig. 6. The reflectivity curve is calculated when the tuning layer is IZO and 100 nm thick.

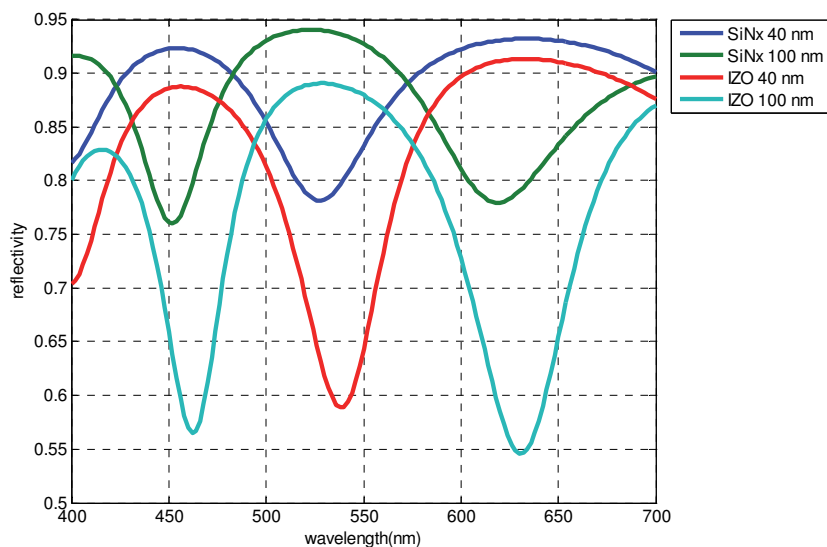


Fig. 7. The reflectivity curves are plotted. The tuning layers are (a) 40 nm SiNx, (b) 100 nm SiNx, (c) 40 nm IZO, and (d) 100 nm IZO, respectively.

Based on this idea, the practical OLED devices were fabricated and demonstrated (Lee et al, 2009a). The schematic diagram of OLED structure with DBR cavities and tuning layers are

illustrated in Fig. 8. We fabricated RGBW AMOLED panels with the above optical designs and the conventional CF used in LCDs (color gamut = 72%). The panels showed a color gamut in the range of 100–110% NTSC. On the other hand, panels with no micro-cavity design had a color gamut of only 75%. Another benefit was increased light output through the CF. With micro-cavity designs, the CF transmission ratio increased to 40% from 27%. The light output from R, G, and B subpixels increased by about 50%.

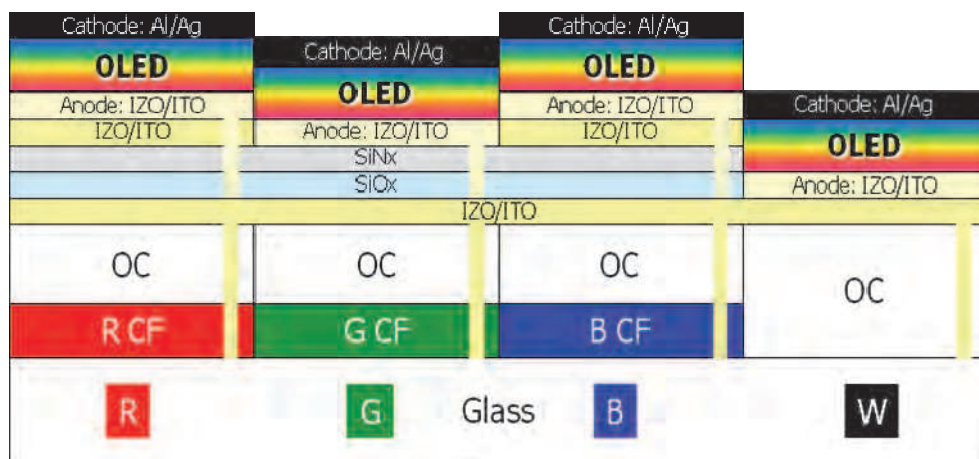


Fig. 8. A micro-cavity design of a RGBW bottom-emitting AMOLED. OC stands for overcoat. The RGB subpixels have DBR (IZO or ITO and SiOx), a filter common for RGB (SiNx), and another filter (IZO or ITO) for R and B subpixels. The W subpixels do not have DBR in order to avoid the spectral modification and dependence on the viewing angle.

#### 4. FDTD analysis for OLED(Lee et al, 2009b)

As matter of fact, the multi-layer theory deals with one dimensional problem since it assume that the physical situation doesn't change for the translation movement in the plane of the layers. This assumption is quite good for the conventional OLED device. The functional layers of submicron thickness are deposited on large area glass, whose lateral dimension is virtually infinite compared to the thickness. However, suppose the OLED structure is made on the curved surface or the wavy substrate for some reason. From this point, the problem becomes two dimensional or three dimensional one, which is not within the scope of multi-layer theory. Then, what kinds of theoretical tools are available to the designer? Even though ray tracing is most frequently used algorithm to calculate the optical property of the system, it lacks capability of handling interference and sub-wavelength feature like thin film. FDTD can be a good option although it takes much time to compute the electric field inside the cavity. The computation time increases rapidly as the feature size and the dimension increases. Therefore, the analysis should be carefully planned to reduce the computation time and obtain the goal of calculation at the same time. In this section we present an example of analyzing the undulated cavity of the OLED structure using FDTD method.

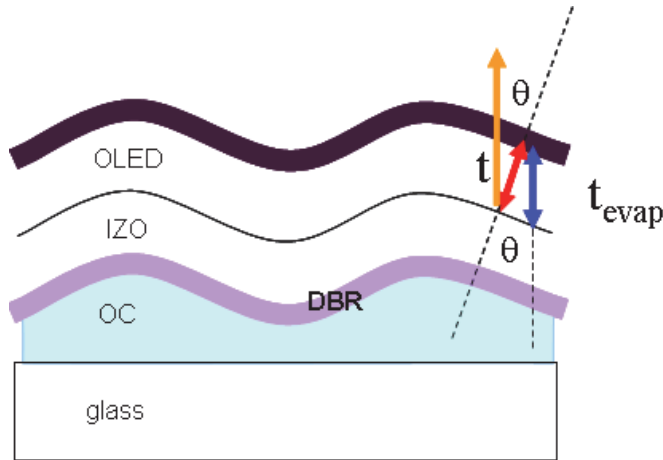


Fig. 9. Principles of tuning resonance in undulated micro-cavity

The main purpose of the undulated micro-cavity is to modify spectrum with the change of undulation profile. The physical mechanism of tuning resonance in undulated cavity is illustrated in Fig. 9. When the OLED layers are deposited over the undulated profile of the overcoat (OC) layer, the thickness of evaporation normal to substrate is uniform over the whole device. However, the thickness normal to the slope is proportional to  $\cos\theta$  if the angle between the slope and the substrate is  $\theta$ . In addition, the emission is not normal to the slope, which leads to the blue shift of resonance peak proportional to the  $\cos\theta$ . As a result, the resonant wavelength of an undulated micro-cavity is proportional to  $\cos^2\theta$ .

The angle of slope is controlled by varying the amount of UV exposure in the lithography process. More UV exposure causes a deeper trench in OC layer after development process. The reflow process smoothen the rectangular profile into a curved surface. In general, the angle of the slope increases as the UV exposure increases. The experimental results are displayed in Fig. 10. The emission peak has changed with the increase of UV exposure time. The red curve represents the micro-cavity tuned to the R and B pixel showing the strong peaks around the red and blue wavelength. The increased UV exposure moves the peak to green wavelength which is optimized for G pixel in OLED display as seen in the brown curve.

In a real device, the UV exposure is controlled by the opening size of the mask pattern. Since the opening size of the mask pattern can be set to different values for RGB pixels, the resonance frequency of each pixel can be tuned simultaneously by one step photolithography. It greatly alleviates the processing burden which typically comes with the micro-cavity devices used for multi-colors.

In order to analyze the resonance shift and other optical properties of an undulated micro-cavity, the FDTD method and the permittivity profile as shown in Fig. 11 were used. In this structure, the micro-cavity largely consists of the organic layers sandwiched between DBR and a cathode. From the bottom-most layer, DBR layers are comprised of 70 nm SiN<sub>x</sub>, 90 nm SiO<sub>2</sub>, 35 nm SiN<sub>x</sub>, 90 nm indium zinc oxide (IZO). The organic layers are 120 nm hole transport layer, 50 nm emission layer, 30 nm electron transport layer. Lastly, the thickness of Aluminum cathode is 200 nm on the top. The region below distributed Bragg reflector (DBR) is assumed to be filled with OC layer. The permittivities used for SiN<sub>x</sub>, SiO<sub>2</sub>, IZO,

hole transport layer, emission layer, electron transport layer and Aluminum are 3.61, 2.25, 4.23, 3.74, 3.51, 2.94 and 0.06+I 3.50 respectively. The undulation profile is modeled using a sine wave form. The period and the height of the sine wave determine the angle of the slope in the undulated micro-cavity.

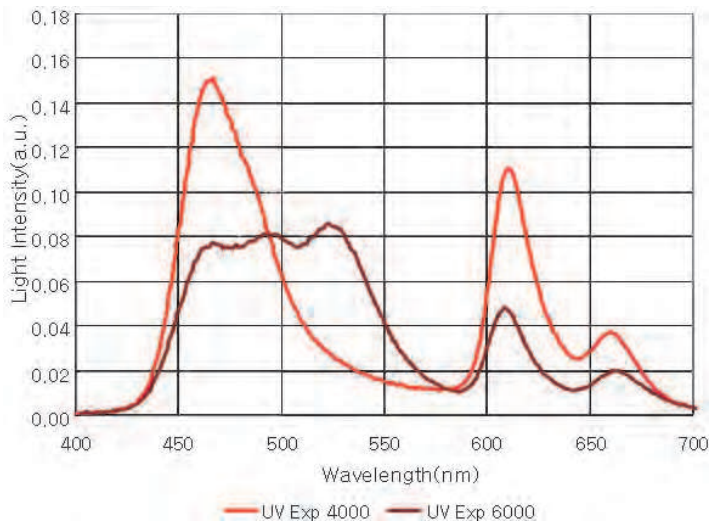


Fig. 10. Emission spectra of white OLED with variation of UV exposure time. The red line and brown line corresponds to 4 s and 6 s of exposure time, respectively.

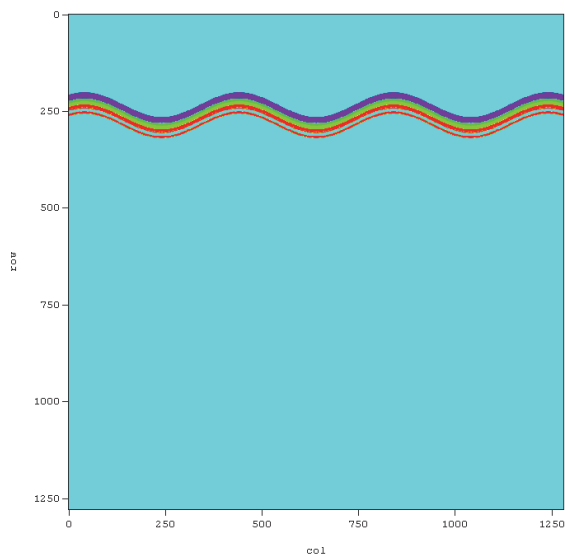
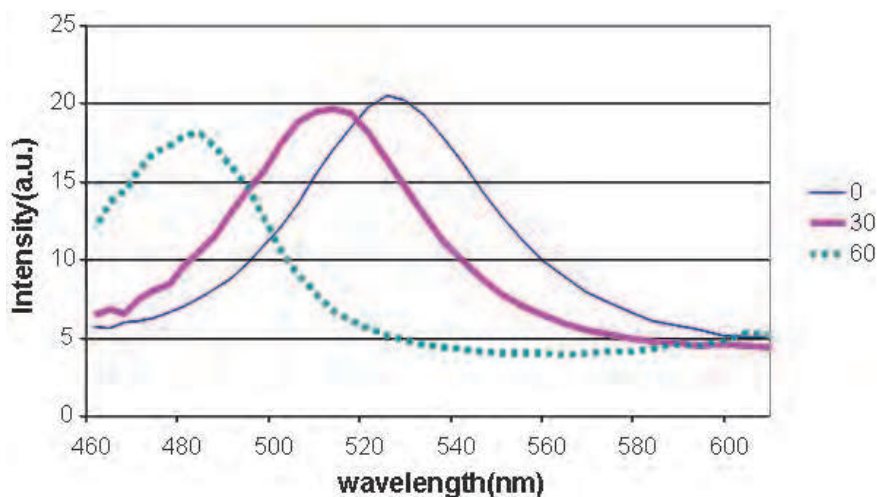
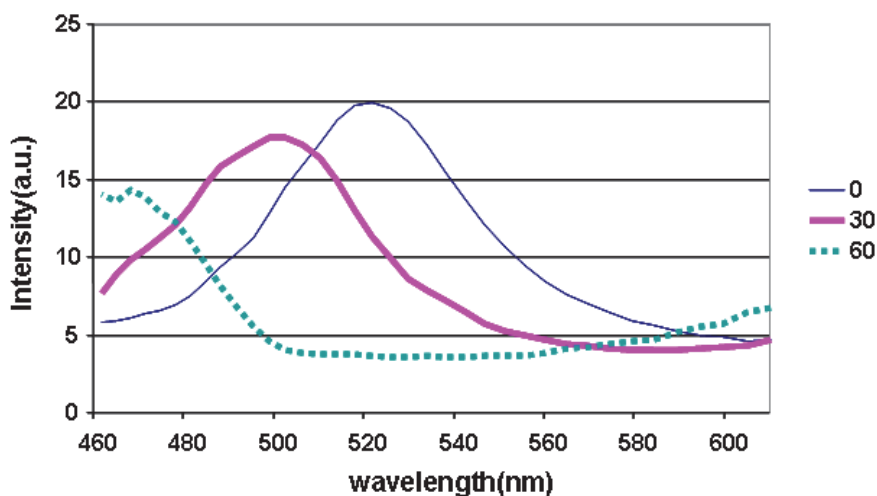


Fig. 11. Permittivity profile of undulated micro-cavity in OLEDs. Period = 5.0  $\mu\text{m}$ , height = 0.6  $\mu\text{m}$ .

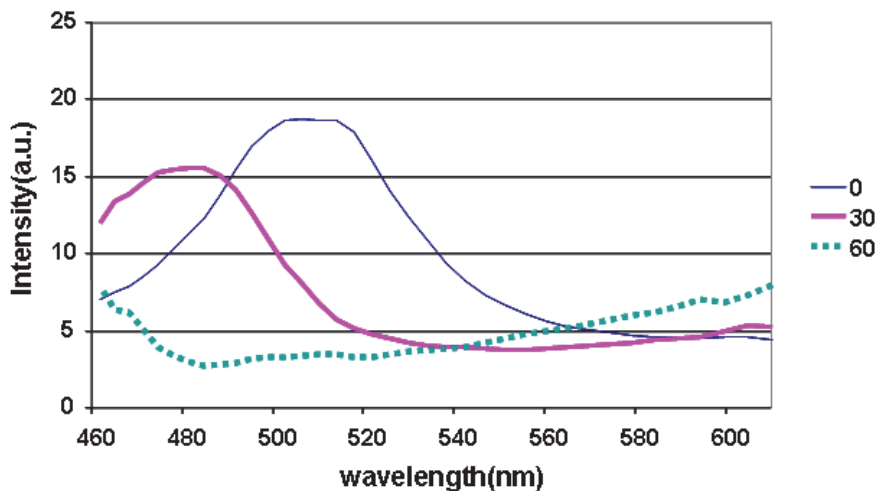
For measuring the spectrum change, the dipole is allowed to oscillate for a short time. Since the short pulse acts as a broad band source, it can be a good light source to characterize the frequency response of the micro-cavity. The detector apart from the dipole source collects the wave emitted at a certain angle. The Fourier transformed output of the collected wave is divided by the Fourier transformed input to give frequency response at each wavelength. In this way, the spectrum change of the micro-cavity can be analyzed.



(a)



(b)



(c)

Fig. 12. Spectrum of dipole emission in undulated micro-cavity with various heights and emission angle; Period = 5.0  $\mu\text{m}$ , height = (a) 0.0  $\mu\text{m}$ , (b) 0.2  $\mu\text{m}$ , and (c) 0.4  $\mu\text{m}$ , emission angle = 0 $^\circ$  (solid), 30 $^\circ$  (thick solid), 60 $^\circ$  (dotted).

When the dipole is placed in the middle of the slope of the undulation profile, the spectrum shows blue shifts as the height increases as seen in Fig. 12. It agrees with the experimental results observed in the real device (Lee et al, 2009a). The dipole is placed in the middle of the slope since the slope region is the brightest part of the device. Thermal evaporation of organic material results in uniform thickness in the vertical direction. It means that the thickness normal to the surface is the smallest near the slope. The reduced thickness of organic layers also reduced the electrical resistance in the part, which leads to the current crowding near the slope. Therefore, locating the dipole in the middle of slope is reasonable to explain the blue shift of the spectrum. Otherwise, the dipole oscillation near peak or valley gives less change to the resonance peak. The resonance peak at normal angle shifts from 525 nm to 510 nm when the height changes from 0.0  $\mu\text{m}$  to 0.4  $\mu\text{m}$ . Since the angle of the slope is roughly 9 degrees at the height of 0.4  $\mu\text{m}$ , the amount of blue shift may be explained by  $\cos^2\theta$  dependence. As explained before, this angle dependency can be ascribed to the layer thinning due to the slanted evaporation and oblique resonance condition, each of which has  $\cos\theta$  dependency. The internal physical mechanisms of undulated micro-cavity that controls the emission wavelength in OLEDs was investigated. The finite-difference-domain method is applied to a previously manufactured OLED design featuring optical structure on a wavy over-coat layer. The emission spectrum shows blue shift of 15 nm when the height of undulation changes from 0.0  $\mu\text{m}$  to 0.4  $\mu\text{m}$  with the period fixed at 5.0  $\mu\text{m}$ . The blue shift is also observed in the experiment and the amount of shift in the simulation complies with  $\cos^2\theta$  dependence.

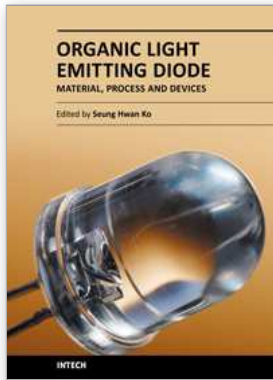
## 5. Acknowledgment

This work was supported by Samsung Electronics Corporation. This work was supported by National Research Foundation of Korea Grant funded by the Korean Government(2009-0071253).

## 6. References

- Born M and Wolf M, *Principles of Optics*, 6th Ed., ISBN 0-02-946146-4, p.55 (1989)
- Fowles G R, *Introduction to Modern Optics*, 2nd Ed., ISBN 0-03-089404-2, Chapter 4 (1975).
- Gasiorowicz S, *Quantum physics*, Chapter 22 (1984)
- Ju Y G, Lofgreen D, Fiore A, Hu S Y, Hegblom E, Louderback D, Sjolund O, Huntington A, Coldren L A, "Densely packed pie shaped vertical-cavity surface-emitting laser array incorporating a tapered one-dimensional wet oxidation", *IEEE Photonics Technology Letters*, vol.12, no. 5, p.462-464, May 30 (2000)
- Lee B W, Ju Y G, Hwang Y I, Lee H Y, Kim C W, Lee J S, and Souk J H, "Micro-cavity design of bottom-emitting AMOLED with white OLED and RGBW color filters for 100% color gamut", *Journal of the Society for Information Display*, Vol. 17, Issue 2, pp. 151-157 (2009a) Feb.
- Lee B W, Ju Y G, "Analysis of undulated micro-cavity in organic light-emitting diodes", *Optical and quantum electronics*, vol. 41, Issue 8, pp. 627-633 (2009b)





## **Organic Light Emitting Diode - Material, Process and Devices**

Edited by Prof. Seung Hwan Ko

ISBN 978-953-307-273-9

Hard cover, 322 pages

**Publisher** InTech

**Published online** 27, July, 2011

**Published in print edition** July, 2011

This book contains a collection of latest research developments on Organic light emitting diodes (OLED). It is a promising new research area that has received a lot of attention in recent years. Here you will find interesting reports on cutting-edge science and technology related to materials, fabrication processes, and real device applications of OLEDs. I hope that the book will lead to systematization of OLED study, creation of new research field and further promotion of OLED technology for the bright future of our society.

### **How to reference**

In order to correctly reference this scholarly work, feel free to copy and paste the following:

Young-Gu Ju (2011). Micro-cavity in organic light-emitting diode, Organic Light Emitting Diode - Material, Process and Devices, Prof. Seung Hwan Ko (Ed.), ISBN: 978-953-307-273-9, InTech, Available from: <http://www.intechopen.com/books/organic-light-emitting-diode-material-process-and-devices/micro-cavity-in-organic-light-emitting-diode>

# **INTECH**

open science | open minds

### **InTech Europe**

University Campus STeP Ri  
Slavka Krautzeka 83/A  
51000 Rijeka, Croatia  
Phone: +385 (51) 770 447  
Fax: +385 (51) 686 166  
[www.intechopen.com](http://www.intechopen.com)

### **InTech China**

Unit 405, Office Block, Hotel Equatorial Shanghai  
No.65, Yan An Road (West), Shanghai, 200040, China  
中国上海市延安西路65号上海国际贵都大饭店办公楼405单元  
Phone: +86-21-62489820  
Fax: +86-21-62489821

© 2011 The Author(s). Licensee IntechOpen. This chapter is distributed under the terms of the [Creative Commons Attribution-NonCommercial-ShareAlike-3.0 License](#), which permits use, distribution and reproduction for non-commercial purposes, provided the original is properly cited and derivative works building on this content are distributed under the same license.